

Extrasolar Planets

By: Steve Strom¹

NOTES: (a) JWST numbers appropriate to the assumptions in their updated Science Requirements Document must be calculated; (b) the GSMT sensitivity calculations must be ‘scrubbed’ to ensure that the assumptions re detectors; atmosphere; emissivity are duly conservative; and (c) the expected performance of the JWST NIR coronagraph needs to be folded in. Please review with these caveats in mind (SES).

More than 100 extrasolar planets are known from radial velocity studies of relatively nearby stars. Over the next decade, the number of detected planets will increase dramatically as a consequence of continued radial velocity and photometric transit studies from the ground, and high precision astrometric measurements from space. By the end of this decade, it is likely that ground-based telescopes, equipped with sophisticated adaptive optics systems will have imaged several extrasolar systems. As we move into the JWST and GSMT era, the challenge will be to *characterize* large samples of extrasolar planets and to understand thereby both their physical and chemical properties and perhaps most significantly, the path or paths that led to their formation.. Both JWST and GSMT have major roles to play in meeting this challenge. The unprecedented mid-IR sensitivity of JWST will enable detection and spectroscopic characterization of planets (a) well separated from their parent stars; and (b) ‘free-floating’ planets. Moreover, JWST will have the power to detect mid-IR spectra of warm planets too close to their parent stars to be resolved. The five-fold increase in angular resolution and 25-fold increase in near-IR sensitivity provided by a 30-m class GSMT will complement JWST by enabling direct imaging and near-IR spectroscopic characterization of planets orbiting stars over a wider range of orbital distances and over a larger volume of space; and (b) near-IR spectroscopic measurements of planets detected and characterized by JWST in the mid-IR.

Background

Over 100 planets orbiting stars other than the Sun have been discovered, the overwhelming majority nearby (at distances < 30 pc) and detected indirectly through the radial velocity (Doppler spectroscopic) technique. These objects range in mass from of order 0.1 to 10 Jupiter masses. Semi-major axes of the detected planets are distributed roughly uniformly from 0.04AU to 5 AU, though the completeness of the sample drops significantly beyond ~1AU. Eccentricities are distributed much like those of binary star systems, with circularity imposed on the closest objects by tidal interaction with the parent stars. In only one case, where the planet transits across the star as seen from the Earth, is the planetary radius determined, and it is roughly consistent with that of a hydrogen-helium (Jovian-type) planet thermally inflated by proximity to the parent star. By extension, then, the vast majority of the Doppler spectroscopic detections—if not all—are extrasolar giant planets (EGPs): bodies like Jupiter orbiting other stars.

Profound questions are raised by the distributions of the orbital elements. Although predictions of giant planet migration, notably by D.N.C. Lin and colleagues, appeared many years before the detection of EGP’s, the potential implications for the semi-major axis distribution of giant planets was not explicitly realized. Post facto, however, the

¹ Much of the input for this document has been provided by Jonathan I. Lunine

semi-major axis distribution of EGP's can be understood in terms of *preferred formation* of the giant planets at or beyond the “ice-line” (the region at which water ice condenses, hence raising the surface density of solids and decreasing accretion time) followed by inward migration.

Alternative to formation in preferred regions of the protoplanetary disk is the possibility that instabilities in massive disks could trigger giant planet formation at most semimajor axes, and that subsequent gravitational interactions in a dynamically “overfull” system would alter orbits and result in ejection of some EGPs (thus creating a population of ‘free-floating’ planets). Formation times much shorter than the disk lifetime are possible in this *disk instability* model.. This model has the further advantage of providing a natural explanation for the observed eccentricity distribution among known EGPs. However, the larger abundance of Jovian mass (up to 10 M_J, roughly) objects compared to more stellar T-dwarfs (or brown dwarfs; 10-80 M_J) does not arise naturally from the disk instability model.

Direct detection and analysis of large samples of EGPs are needed in order to understand their nature and how they were formed. Both JWST and GSMT have key roles to play in making the required measurements, which are of significant astrophysical interest in their own right, and essential to learning whether systems like our own solar system -- in which the inner region is devoid of giant planets and hence dynamically available for rocky terrestrial planets – are rare or common.

Discriminating between EGP Formation Scenarios

There is a potential discriminant between EGP formation (a) in preferred zones; and (b) via disk instability: the metallicity contrast between the planet and its parent star. A formation model that favors growth at and beyond the disk ice line is based on modeling the growth of giant planets in relatively quiescent, less-massive disks. Under such conditions significant addition of gas to make a giant planet does not occur until initial accretion of a rocky and icy core seeds the collapse of gas. As the gas is added, more solids from the surrounds fall into the growing giant planet – thus producing an EGP having significantly higher metallicity than its parent star. This model explains both the high metallicity of Jupiter and Saturn relative to the Sun as well as the distribution of heavy elements throughout the interior, not just in the core. Conversely, the disk instability model requires conditions such that addition of rocky and icy material in significant amounts to the rapidly-formed protoplanets is unlikely. Such a model cannot readily explain the metallicity of Jupiter and Saturn (both of which create additional difficulties for the disk instability model, including how one forms a regular satellite system in the process).

Observations of metal abundances in EGP atmospheres could potentially enable determination of the fraction that form via the disk instability process and the fraction that form analogously to Jupiter and Saturn. *Those formed via disk instability would have metallicities similar to that of their parent stars, while EGPs formed by core formation and slow accretion should be significantly enriched.*

Analyzing EGPs: Lessons from Brown Dwarf Studies, Jupiter and Saturn

Considerable experience in analyzing the spectra of substellar objects has been accumulated since 1995, when the first definitive brown dwarf was discovered. A well-quantified extension of the stellar spectral sequence below the M-dwarf range (to so-called L- and T-dwarfs has been possible largely as a consequence of ground-based surveys (2-MASS and Sloan). The bottom of the T-dwarf subclass lies at an effective temperature of 800 K, above the range of all EGPs except for the most massive, youngest, or most proximate to the parent star (figure 1). Distinguishing objects later than the T-dwarf sequence, which we shall call EGPs without prejudice regarding brown dwarf vs. planet formation mechanisms, are (a) water and ammonia cloud formation; (b) strength of methane absorption features; (c) disappearance of the strong alkali metal features around 1 micron wavelength; (d) reversal of the J-K color from a bluing to a reddening with decreasing effective temperature, and (e) a precipitous drop in the flux shortward of 4 microns. This list applies as well to isolated, free-floating EGPs, or EGPs located far from their parent stars ($d \gg 5$ AU). For bound EGP's close enough to the parent star that stellar photons dominate in the near-infrared, the precipitous drop in near-IR flux is replaced by an entirely reflected component, and some of the other indicators change as well (figure 2).

While the EGP realm represents unexplored terrain, the experience gained from Jupiter/Saturn, L- and T-dwarfs provides some confidence that we can predict fluxes vs. wavelength in the effective temperature *terra incognita* from 800K down through 130 K. Major uncertainties include the role of clouds in damping the strong infrared excess in the 5 micron region, and the effects of stratospheric emissions and day-night temperature differences on bound EGPs. Minor uncertainties concern the details of the line absorption coefficients for individual molecules used to build the gaseous molecular component of the model spectra. Nonetheless, armed with results from these models, and later, analysis of large samples of L and T dwarfs spanning a range of temperatures, we can predict brightnesses and detectability of EGPs, and as well suggest that metallicities can be derived from moderate resolution ($R=1000$) spectra to provide a potential constraint on formation models. In the following section, we describe key measurements needed to characterize EGPs. Quantitative flux estimates are based on the assumption that EGPs are located at a standard distance of 10 parsecs.

Key Measurements Needed to Characterize EGPs

1. Detection and analysis of free-floating EGPs.

Figures 3 and 4 illustrate that detection of a 1 M_J EGP 100 million years old and a 5M_J EGP 5 billion years old are possible with a 30-m class ground-based telescope. However, the latter is too faint for comprehensive spectroscopy; indeed, its detectability depends upon the excess flux in the 5 micron region. The young Jupiter mass object, on the other hand, can be analyzed spectroscopically at selected wavelengths. Younger or more

massive objects, will of course be easier targets; these two examples represent part of the defining envelope of detectability/analyzability for isolated EGPs in the near-infrared.

II. Detection and analysis of bound EGPs.

For bound systems the crucial parameters determining detectability are the contrast ratio of the planet relative to the star, and the angular separation between the two. Either coronagraphy or interferometry are required to pull the light of the planet out from behind the glare of the parent star. Of crucial advantage is large telescope aperture in order to minimize the angular extent of the bright fringes of the parent star at the location of likely planetary companions. GSMT will feature a very large mirror diameter, which coupled with advanced coronagraphs on the telescope should enable detection of bound EGPs. Figure 5 plots the model contrast ratio of planet to star versus wavelength for the system 55 Cnc, in which two planets have been detected by the Doppler spectroscopic method. The closer planet, 55 Cnc b, is both warmer and more heavily irradiated than 55 Cnc d, and has contrast ratios generally between 10^{-6} and 10^{-4} in the near-infrared to mid-infrared. However, its angular separation from the star as seen from Earth is less than 0.01 arcseconds, making it an impractical candidate for coronagraphic or interferometric techniques. The contrast ratio for 55 Cnc d is everywhere less than 10^{-7} except in the 5 micron peak and beyond 10 microns. Coronagraphs and AO systems currently under design for 20-30m telescopes promise to detect point sources at contrast ratios 10^{-7} to 10^{-8} at angular separations $\theta > 5 \lambda/D$. At a wavelength of 5 microns, 55 Cnc d ($\theta = 0.45''$) should be well resolved with a 30-m diameter GSMT.

Figure 6 shows that the absolute flux of 55 Cnc d, an object > 4 Jupiter masses, exceeds the sensitivity limit for GSMT photometry. Thus, this planet is a candidate for direct detection, though not necessarily spectroscopy, by GSMT. A handful of the known EGP cohort fall into this detectable category. Others will likely be discovered soon by Doppler spectroscopic techniques, and GSMT itself could search candidate stars at larger semi-major axes to make direct detection discoveries.

Comparison with JWST

GSMT will be the dominant facility for the detection and spectroscopy of isolated EGPs through the 5 micron wavelength region, with JWST doing a better job beyond 5 microns. The ability to detect spectral features across a wide range of wavelengths from the two facilities will provide stronger constraints on abundances, on the effects of clouds on a particular object, and (for R=1000 spectroscopy) the surface gravity. The detectability of EGPs increases dramatically in the infrared, which allows JWST to compensate for its smaller aperture relative to GSMT.

For bound systems, even though the contrast ratio is better beyond 5-10 microns than it is shortward, more sophisticated coronagraphy and the much smaller diffraction limit of GSMT compared with JWST will be key to detecting and characterizing EGPs at typical separations around nearby stars of $0.5''$ - $1''$ (5 to 10 AU at a distance of 10 pc). JWST will be the instrument of choice for EGPs located at distances beyond 10 AU (at 10 pc)

provided that the planetary effective temperature is large enough to ensure detection of the thermal radiation.

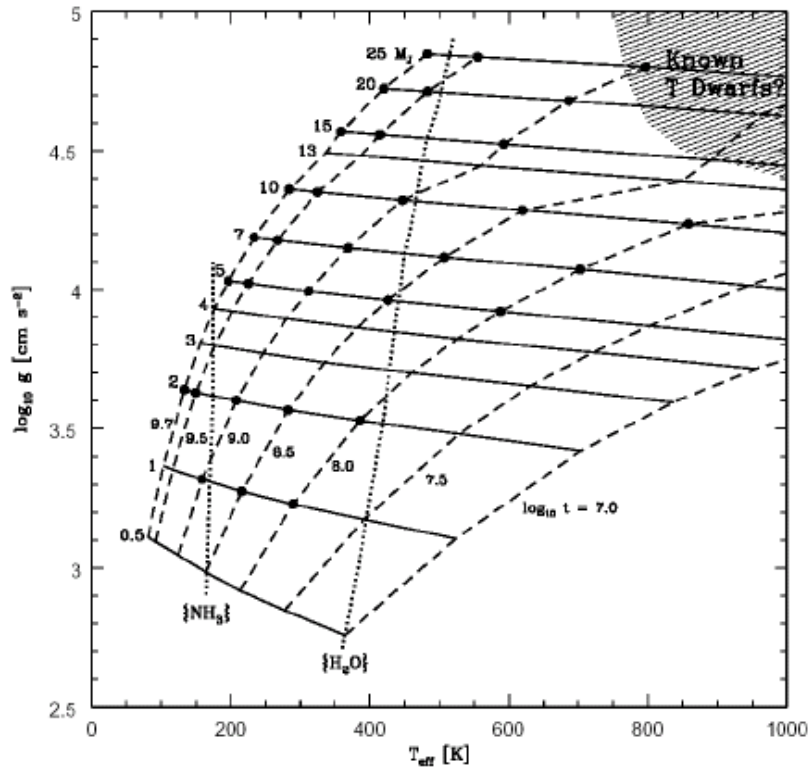


Figure 1. Surface gravity versus effective temperature (logarithmic) for isolated EGP's. Lines of constant mass and lines of constant age (logarithmic, years) define the grid for the solar composition objects modeled here. The realm of the coolest T-dwarfs occupies the upper right corner, with a minimum effective temperature of 740-800 K. Dashed lines demarcate the onset of water cloud and ammonia cloud formation near the unity optical depth level in the atmospheres. Bound EGP's will depart progressively from this grid according to the flux of energy they receive from their parent star. From Burrows et al. (2003).

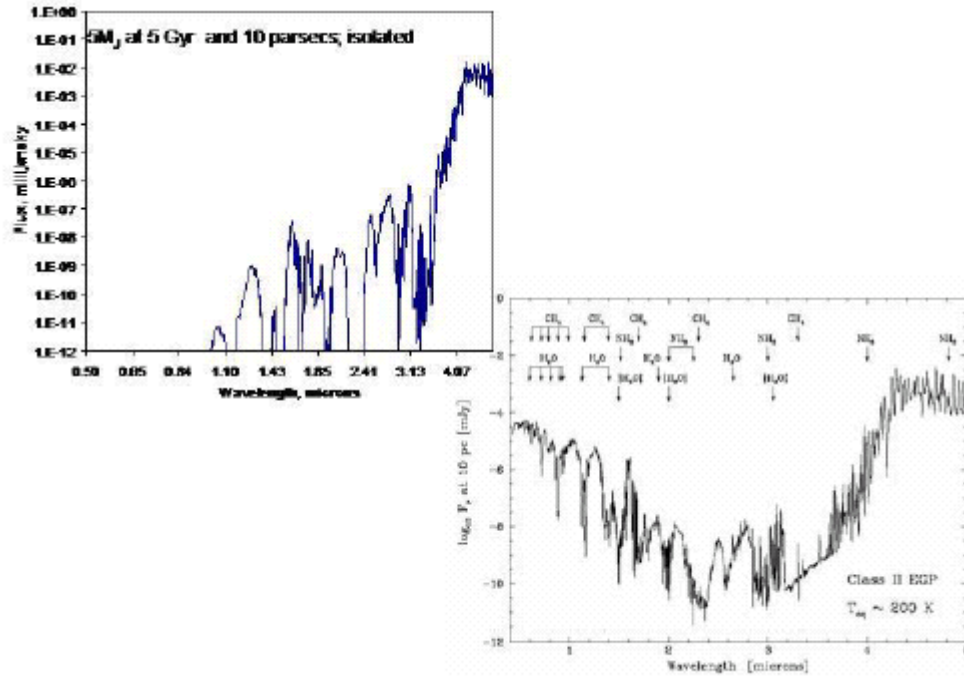


Figure 2. Comparison of EGP's with roughly the same effective temperature. Top model is an isolated object; bottom model is a bound EGP some 1-2AU from a solar-type star. Both plots are flux at Earth (millijansky) versus wavelength in microns. The reflected stellar light for the bound EGP fills in the flux in the region shortward of 2 microns. Models from Burrows et al. 2003 (top) and Sudarsky et al. 2003 (bottom).

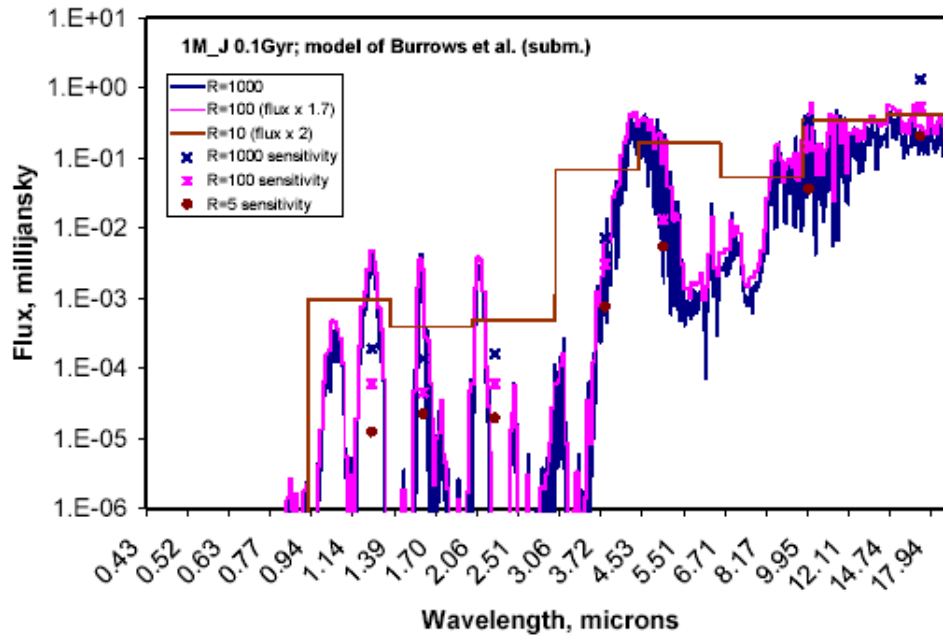


Figure 3. Flux (millijansky) at Earth vs. wavelength (microns) for a one Jupiter mass EGP at 10^8 years of age, 10 parsecs distance, isolated. Spectra for $R = 1000$, 100, and 10 are shown (the latter two displaced for clarity) along with corresponding GSMT sensitivities, displaced in proportion to the corresponding spectra. GSMT sensitivities, courtesy M. Mountain, are for a 10^4 second exposure, $S/N=10$, with 4×4 pixels across the point source, an assumed GSMT emissivity of 10%, and a telescope diameter of 30-m.

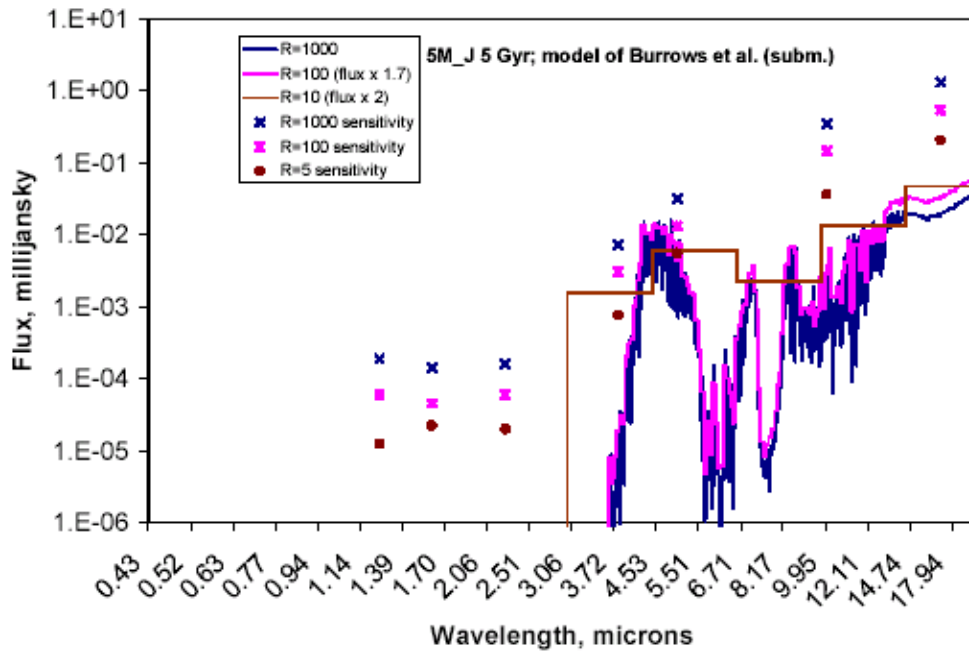


Figure 4. Same as figure 3, for a 5MJ isolated EGP at 5×10^9 years.

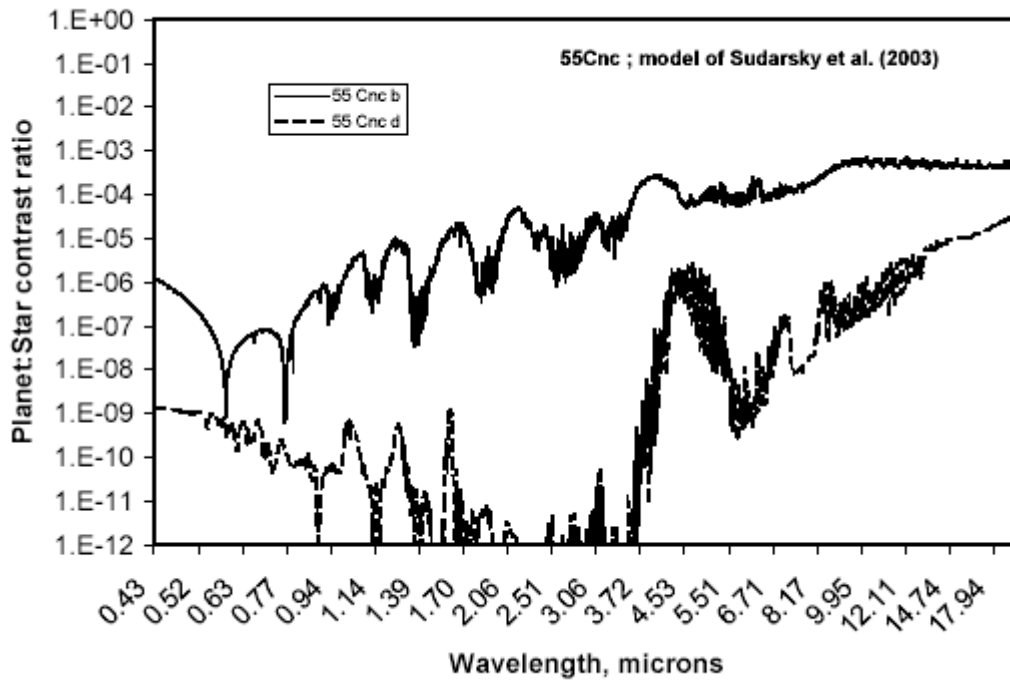


Figure 5. Contrast ratio of the flux from the planet relative to the star for the two EGP's in the system 55 Cnc.

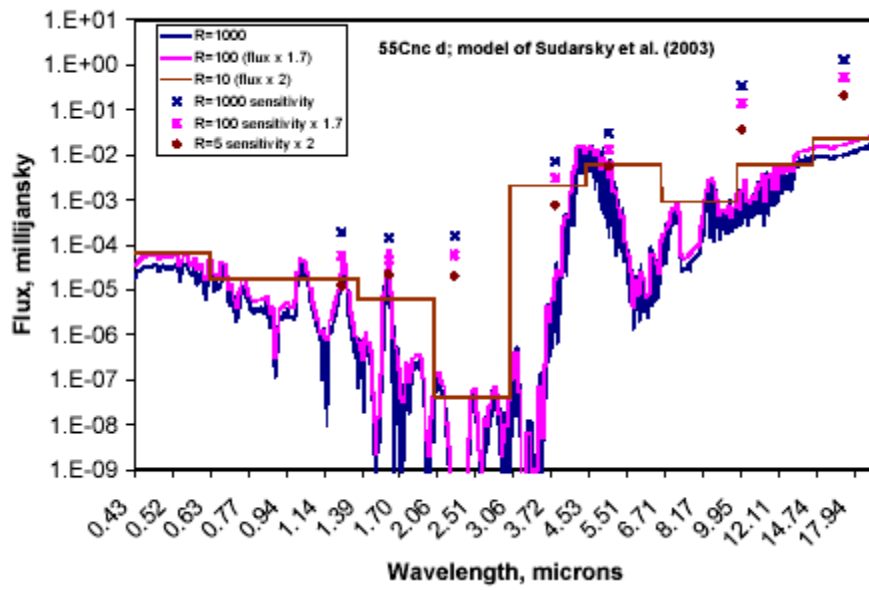


Figure 6. Flux versus wavelength for 55 Cnc d, for three spectral resolutions (displaced from each other for clarity) and corresponding sensitivities. For R=5 the EGP, if separable from the parent star (see figure 5) can be detected with a 30-m class GSMT.

Detectability of Extrasolar Giant Planets: Summary

[NOTE: THIS SECTION STILL NEEDS CORRESPONDING JWST NUMBERS!]

The models summarized above can be used to predict the limiting distance to which extrasolar giant planets can be detected. Our working assumptions are summarized in Table 1 in which we list the limiting fluxes (nJy) for the indicated wavelengths and spectral resolving powers and a signal/noise ratio of 25 per resolution element. A 30-m GSMT with 10% emissivity is assumed.

Table 1: Limiting Fluxes (nJy) to reach S/N =25 in the indicated integration times

λ (μ)	<u>R=10</u>		<u>R=100</u>		<u>R=1000</u>	
	10^4 sec	10^5 sec	10^4 sec	10^5 sec	10^4 sec	10^5 sec
1.25	8.9 nJy	2.8	42	12	250	67
2.25	38	12	86	27	380	110
3.8	1300	420	4500	1400	18000	5800
4.6	8700	2900	17000	5800	50000	17000

Tables 2 lists the planet fluxes estimated from the models described above, while Tables 3 through 6 summarize the limiting distances to which a given planet could be observed by a 30m GSMT.

Table 2: Fluxes (nJ) for Selected Extrasolar Giant Planets

Planet	1.25 μ	2.25 μ	3.8 μ	4.6 μ
1 M _j 100 Myr	3000	2000	8000	10^5
2 M _j 100 Myr	10^5	5×10^4	10^4	3×10^5
1 M _j 5 Gyr 1.5 AU	6	10^{-5}	0.01	1000
1 M _j 5 Gyr 5 AU	69	1	8	1.1×10^4

Table 3: Limiting Distances to which a 1 M_J planet of age 100 Myr can be observed

λ (μ)	<u>R=10</u>		<u>R=100</u>		<u>R=1000</u>	
	10 ⁴ sec	10 ⁵ sec	10 ⁴ sec	10 ⁵ sec	10 ⁴ sec	10 ⁵ sec
1.25	183pc	327	84	158	35	67
2.25	72	129	48	86	23	43
3.8	24	44	13	24	7	12
4.6	34	58	24	41	14	24

Table 4: Limiting Distances to which a 2 M_J planet of age 100 Myr can be observed

λ (μ)	<u>R=10</u>		<u>R=100</u>		<u>R=1000</u>	
	10 ⁴ sec	10 ⁵ sec	10 ⁴ sec	10 ⁵ sec	10 ⁴ sec	10 ⁵ sec
1.25	1060pc	1889	487	912	200	386
2.25	362	645	241	430	115	213
3.8	28	49	15	27	7	13
4.6	58	101	42	72	25	42

Table 5: Limiting Distances to which a 1 M_J planet located at 1.5 AU of age 5 Gyr can be observed

λ (μ)	<u>R=10</u>		<u>R=100</u>		<u>R=1000</u>	
	10 ⁴ sec	10 ⁵ sec	10 ⁴ sec	10 ⁵ sec	10 ⁴ sec	10 ⁵ sec
1.25 8	pc	14	3.8	7	1.5	3
2.25	ND	ND	ND	ND	ND	ND
3.8	ND	ND	ND	ND	ND	ND
4.6	3.4	6	2.4	4	1.4	2.4

Table 6 Limiting Distances to which a 1 M_J planet located at 5 AU of age 5 Gyr can be observed

$\lambda(\mu)$	<u>R=10</u>		<u>R=100</u>		<u>R=1000</u>	
	10 ⁴ sec	10 ⁵ sec	10 ⁴ sec	10 ⁵ sec	10 ⁴ sec	10 ⁵ sec
1.25	27 pc	49	13	24	5.2	10
2.25	1.6	2.9	ND	1.9	ND	ND
3.8	ND	1.4	ND	ND	ND	ND
4.6	11	19	8	14	4.7	8

We conclude that Jovian mass planets of age 100 Myr can be detected and characterized (at $R \sim 100$) out to the TW Hydra association, provided that they can be separated from their parent star. Detection of ‘old, cold’ Jupiters will be restricted to the immediate solar neighborhood.